Experimental optimization of the hundred-keV electron source from laser-driven wire target

Yushan Zeng[1,2], Chuliang Zhou[1,2], Rong Qi[1], Zhongpeng Li[1,2], Haiyi Sun[1], Ye Tian[1,2] (ID), Jiansheng Liu[1,3] and Zhizhan Xu[1,2]

[1]State Key Laboratory of High Field Laser Physics, Shanghai Institute of Optics and Fine Mechanics, Chinese Academy of Sciences, Shanghai 201800, P. R. China; [2]Center of Materials Science and Optoelectronics Engineering, University of Chinese Academy of Sciences, Beijing 100049, P. R. China and [3]Department of Physics, Shanghai Normal University, Shanghai 200234, P. R. China

Abstract

We present the experimental optimization of electrons in the several hundred keV energy range originated from laser-irradiated wire targets. Accelerated by a femtosecond laser pulse, an electron pulse emitted from the wire target was collimated immediately along the wire to a filter unit for the manipulation of energy and spatial distributions. It is shown in simulation that with a pair of magnets as the filter unit, the optimized electrons could serve as a compact and tunable electron source. The proposed system was demonstrated in a proof-of-principle experiment where we attained 1 fC bunch charge with transverse coherence length approaching 1 nm based on a 0.2 TW laser platform. This indicates the scheme as a promising candidate for single-shot electron diffraction.

Introduction

In the last few decades, laser-wakefield acceleration (LWFA) has been a vibrant research area for its successful application in low emittance electron beam generation in the gigaelectron volts (GeV) scale (Malka *et al.*, 2006; Wang *et al.*, 2013; Leemans *et al.*, 2014; Couperus *et al.*, 2017; Dann *et al.*, 2019). However, for the most modest lab scale and portable applications like field manipulation of electrons and ultrafast electron diffraction (UED) (Srinivasan *et al.*, 2003; Calendron *et al.*, 2018; Schaeffer *et al.*, 2018), a compact, relatively inexpensive, high average current source of laser-accelerated electrons is sufficient and much desirable.

Another crucial problem of electron source is related to the beam charge. Take UED for example, large electron charge becomes particularly important since the detection of many irreversible ultrafast processes require high-brightness electrons in one single shot. Whereas the conventional methods for generating ultrafast electron source generally follow a two-step method: firstly, femtosecond laser pulses is used to generate electron pulses from photocathode; then, the generated electron pulses are accelerated by an external static electric field with the field strength up to several tens of kilovolts (Harb *et al.*, 2008; Sciaini and Miller, 2011). The pulse charge is often limited to the order of only 1 fC in order to minimize the pulse duration broadened by space charge forces, making it almost impossible to perform single-shot measurements with such a low-brightness electron pulse. For electron diffraction in the MeV range, on the other hand, such a high-energy electron source is limited to transmission mode only owing to the picometer-size electron wavelength and the small few mrad diffraction angle (Musumeci *et al.*, 2010). In addition, MeV energy range also suffers from other disadvantages such as small cross section of elastic scattering and high radiation damage to samples (Tokita *et al.*, 2009; Gulde *et al.*, 2014). For electrons in hundreds keV energy range, pulse-compressed electrons have been developed to supply hundreds of fC electron charge utilizing radiofrequency (RF) wave to compress the beam pulse. But it also suffers from the big size of the facility and the time jitter between electron beam and RF wave (van Oudheusden *et al.*, 2010; Otto *et al.*, 2017).

In contrast to photocathode or gas plasma, the laser solid-density plasma interaction benefits from its high laser absorption efficiency (Thévenet *et al.*, 2015) and could supply a few nanocoulomb electrons in a single shot. The laser-driven electron sources, thus, show great advantages in terms of brightness when compared with a conventional photocathode-based electron source. However, the heating mechanisms that underly such electron sources like resonant absorption, vacuum heating, $J \times B$ heating, and stochastic heating (Gibbon, 2004) also give rise to large divergence angles and quasi-thermal broad energy spectra (Mordovanakis *et al.*, 2009; Tian *et al.*, 2012). Directional electron beams have been produced via vacuum laser acceleration with a plasma mirror injector (Thévenet *et al.*, 2015). Unfortunately, the beam collimation also suffers from the ponderomotive force of the laser pulse in vacuum during acceleration, which results in a large divergence angle (hundreds of milliradians) and a

halo in the electron beam profile. As a result, despite several attempts have been made to employ laser-accelerated electrons from solid targets as the electron source for UED use, the relatively low electron charge still renders these schemes fall short of an ideal source for UED (Tokita *et al.*, 2009, 2010).

In this paper, we present experimentally an optimized electron source form laser-driven wire target. In contrast to the planar solid targets, electrons accelerated from wire targets experience a radial field immediately established on the target surface and gyrate along the wire surface in a helical manner (Tokita *et al.*, 2011; Nakajima *et al.*, 2013; Tian *et al.*, 2017). Many electron pulse can, hence, be strongly concentrated and harnessed to form a compact and collimated electron source. By combining the laser-irradiated wire target and an electron filter unit, we develop a simple system that could serve as a convenient electron source with potential for single-shot electron diffraction. Our scheme embraces both the merits of compactness and potential high charge comparable to those based on LWFA.

Methods

Concept and implementation

The experimental implementation of our laser wire-based electron diffraction device is schematically depicted in Figure 1a and consists of two functional units: one for electron pulse generation and one for filtering electrons that would satisfy the demand of single-shot electron diffraction. In general, the laser–solid interaction could result in a rather wide energy spectrum. As a result, to achieve the desirable electron beam for electron diffraction, a component responsible for narrowing energy spread is indispensable. Here, a pair of dipole magnets and several apertures are utilized to narrow the energy and angular spread in the proposed scheme. The collimated electrons from the target are spatially filtered by an entrance aperture and guided to the pair of dipole magnets, which allow the wire target to traverse it. In the dipole magnets, the path of electrons with different energy deviates. And a filter tube comprised of two apertures in the exit of the magnets therefore enables the spatial as well as energy filter of the electrons.

To effectively optimize the filtered electron beam in terms of electron charge and transverse coherence that determine the diffraction image quality, the magnets could adjust in field strength as well as their separated distance. For energy separation using the magnet pairs, neighboring magnets are set to identical magnetic field strength with opposite direction and the following filter tube is optically aligned by a small He–Ne laser beam parallel to the wire. Since a vast number of electrons from the laser–solid interaction (up to hundreds of pC or even a few nC, depending on the laser intensity) are collimated into the first magnet by the wire target regardless of energy difference, a tailored filter tube would keep enough electron charge for single-shot electron diffraction with adequate transverse coherence. In this work, electron pulse that enters the entrance hole of the first magnet carries approximately ~10 pC electron charge. However, a significant improvement in electron charge, as well as divergence angle, could be expected when a laser pulse of large intensity is applied. Electron charges of several hundred pC and even over a few nC in the center spot have been reported when applying 5×10^{18} and $\sim 10^{19}$ W/cm^2 pulse intensity, respectively (Tokita *et al.*, 2011; Nakajima *et al.*, 2013), while simultaneously, most of the electron energy still falls in the range of around 100–300 keV. In such

scenario of several nC initial charge, a mere 0.001% portion of the electrons filtered out could satisfy the electron charge demand of an ideal diffraction electron source (van Oudheusden *et al.*, 2007).

Laser-driven electron collimation along the wire target

Laser–solid interaction at relativistic intensities produces substantial fast electrons in the sub-MeV range. A small fraction of the hot electrons is emitted into the vacuum and give rise to a charge-neutralizing disturbance propagating away from the interaction region. An interesting case to consider is the wire target. Once applied to a wire target, a transient radial charging field would be generated by this sudden charge separation, which could, in turn, drive back the ejected electrons to move along the wire. With adequate laser intensity, the electric field of the transient field has been experimentally demonstrated its capability of transporting electrons along the wire surface over a distance as far as over 1 m (Nakajima *et al.*, 2013). Electrons emitted from wire targets are thus far more concentrated in space than planar targets.

For diffraction utility, an image plate (IP; Fujifilm BAS-SR2025) placed opposite the wire allows assessing of the electron distribution and charge amount. The electron pattern in Figure 1b shows a typical image taken at a traveling distance of 40 mm from the irradiated spot. Electron emission angle and dose distribution can thereby be retrieved from the pattern. Figure 1c displays the three-dimensional dose map of the electron beam. Since the most of these electrons are constricted in close vicinity to the wire with a small divergence angle, a blocking aperture is placed in the entrance of the filter stage to preclude the influx of outer electrons and meanwhile modulate the divergence of the electrons that are allowed in.

### Electron filter approach: analytical description by the transverse coherence length

For experimental validation of the proposed scheme, the spatial resolution of the electron source for diffraction is quantified by the transverse coherence length L_c as follows (van Oudheusden *et al.*, 2007):

$$L_c = \frac{\hbar}{mc} \frac{\sigma_x}{\varepsilon_{n,x}}, \tag{1}$$

where m is the electron mass, c is the speed of light, $\hbar$ is Planck's constant, σ_x is the rms bunch radius, and $\varepsilon_{n,x}$ is transverse normalized emittance. At the sample, the transverse coherence length L_c of at least several unit cell dimension is required to ensure good quality of the diffraction pattern. A radical increase in L_c can be achieved by lengthening the filter tube or using a smaller radius, though at the dispense of a shrinking electron number. As a result, the trade-off between electron charge and the transverse coherence length is made by carefully adjust the magnets as well as the shape (namely its length, radius, and distance related to the wire) of the filter tube with the help of particle tracing simulations.

Simulation

Numerical simulations of the electron beam were carried out for electron beam optimization in the filter stage using particle tracking code ELEGANT (Borland, 2000). The space charge effect was ignored in the simulation. Emitted electrons from the laser–wire
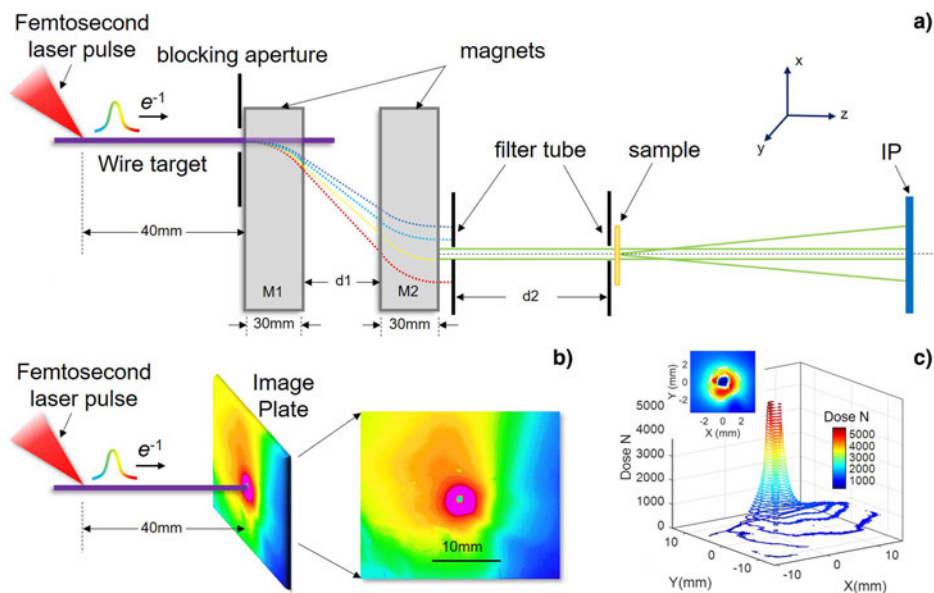
Fig. 1. Schematic representation of the proposed setup for electron diffraction using laser-irradiated wire target. (a) A pair of magnets and several apertures function as the electron filter. (b) Schematic of the layout for measuring electrons at the entrance of the magnets. The obtained single-shot saturated ring zone on the IP indicates a vast number of electrons collimated in a small divergence by the wire target. (c) Three-dimensional profile of the electron beam near the wire target corresponding to the data obtained in (b) with dose N in electrons/0.04 mm^2, where the inset shows the two-dimensional dose map of the central part of the beam. The dashed white circle in the inset represents the half-maximum height contour of the beam.

interaction were approximated by the Gaussian distribution with initial full-width at half-maximum (FWHM) spatial size and temporal span hypothesized to be identical to the laser pulse. It is assumed in the simulation that the electron beam produced at the laser spot has a uniform energy and angular distribution. Also, helical movement is not included in the simulation here because, on the one hand, the angular momentum of the filtered electrons is rather small when compared to the forward momentum. On the other hand, the emittance of the selected electrons from after the whole filter system is determined by the filter tube at the end of the system which further undermines the effect brought by the helical motion. In accordance to the experimental results under present laser and wire parameters, the initial electron beam was set with a momentum distribution of peak momentum of 419 keV/c ($E = 150$ keV) and an FWHM $\delta p/p = 33\%$. When the entrance blocking aperture has a diameter of 3 mm, the electron beam that enters the first magnet has a root-mean-square (rms) radius of 1.06 mm.

The optimized position of the first magnet, at $z = 40$ mm, has been chosen such that the small portion of energetic electrons with broad emitting angle is stopped by the first aperture from entering the filter unit. The two magnets have a width of 30 mm, whereas their magnetic field strength and separation distance are chosen in accordance with the quality of the injected electron beam. The quality of the filtered electron beam is determined by a combined action of the magnets and filter tube. Longer tube length with narrow radius contributes to smaller transverse emittance and energy spread though at the cost of a reduction in electron number. When aiming for single-shot diffraction with a transverse coherence length of $L_c \geq 1$ nm, about 0.1 pC charge is necessary for sufficient diffraction quality (Tao *et al.*, 2012).

Figure 2 shows the bunch evolution in the optimized setup for selected energy of 150 and 250 keV. The locations of the magnets and the filter tube are also shown in the figure. For energy selection of 150 and 250 keV, magnetstrengths are respectively set to 25 and 20 mT. The second magnet M2 is located contiguous to the M1 ($d1 = 0$ mm) in both cases and produces an equal magnetic field with M1 but in the reversed direction. When leaving the magnets, the bunch emittance drops abruptly in the filter

tube by several order of magnitude to 10^{-2} due to the energy filter by the magnets and filter tube. Here, filter tubes of 0.3 mm diameter, length $d2 = 150$ mm and 0.4 mm diameter, length $d2 = 250$ mm are used, respectively, for 150 and 250 keV energy selection. Snapshots of the phase-space distribution in transverse x–y plane, phase-space, and the longitudinal phase-space at the sample place are plotted in Figure 3.

We list the beam parameters at the sample position for both 150 and 250 keV in Table 1. At the sample, the filtered bunch for 150 keV is characterized by a transverse rms size of 0.22 mm, a normalized emittance of 0.04 mm mrad, a relative rms momentum spread of 1.1%, and a transverse coherence length of 1.1 nm. The portion of filtered electrons is 0.004% of the initial electrons. Similar results are produced with 250 keV energy though with less portion of 0.002% filtered out. If the initial bunch charge carries a few nC, the filtered electron charge could thereby well satisfy the charge demand for single-shot electron diffraction.

Experimental results and discussion

To experimentally demonstrate the proposed scheme, proof-of-principle experiments are conducted with the setup shown schematically in Figure 1a. A *p*-polarized laser pulse (central wavelength at 800 nm with FWHM pulse duration of 30 fs) from a commercial 1 kHz Ti:sapphire chirped-pulse amplifier with an 8 mJ pulse energy was focused to an FWHM spot diameter of 4 µm ($1/e^2$) by an $f/2$ off-axis parabolic mirror. Taking into consideration of the 60% propagation loss is in our laser path and 70% pulse energy within FWHM radius, it yields a peak intensity of approximate 5×10^{17} W/cm^2 on the tungsten wire target (50 µm diameter) at an incident angle of 45° (in the x–z plane on Figure 1, where laser path and wire axis are aligned on the same height). Amplified spontaneous emission is measured to be less than 10^{-6} of the peak intensity of the laser pulses. The wire target is mounted with one end fixed on a motor and the other end tightened by a small weight. As a result, laser damage to the wire could be ignored since the wire can be moved by the motor to avoid irradiation on the same spot. The whole setup is placed in a vacuum chamber with pressure under 0.1 Pa.
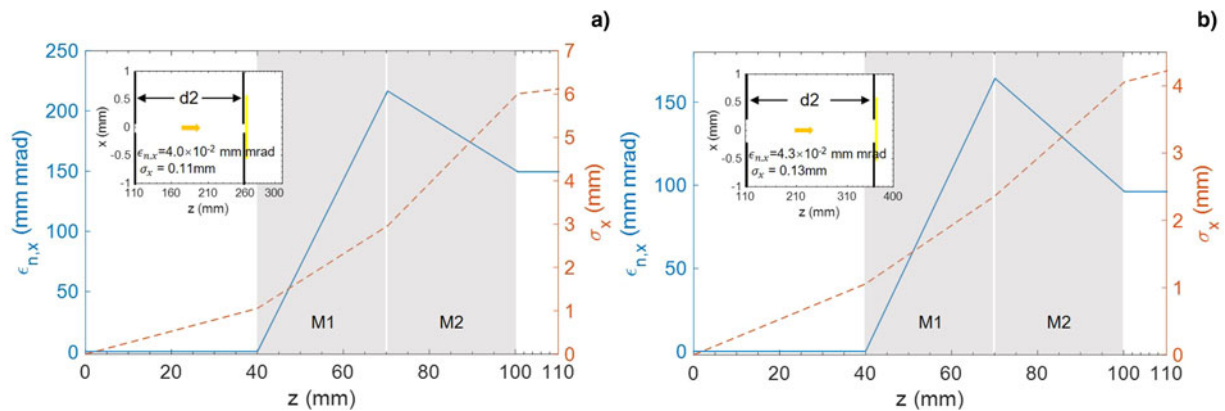
Fig. 2. The bunch transverse normalized emittance $\varepsilon_{n,x}$ (solid line) and rms radius σ_x (dashed line) evolution in the optimized filter unit for selected energy of (a) 150 and (b) 250 keV. The insets present the layout of the filter tube with the outcome $\varepsilon_{n,x}$ and σ_x.
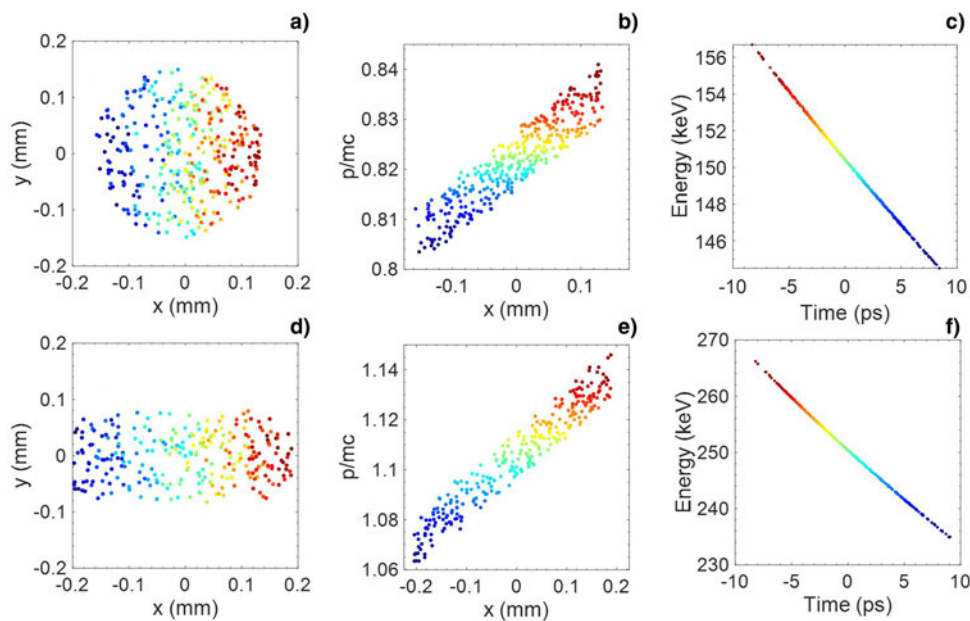
Fig. 3. (a–f) Phase-space distribution projections for selected energy of 150 (row 1) and 250 keV (row 2). The distribution is color-coded by energy with blue to red for lower to higher energies.

Table 1. The filtered beam parameters for selected energy of 150 and 250 keV

	150 keV	250 keV
Rms momentum spread (%)	1.1	1.6
Normalized rms emittance (mm mrad)	0.04	0.04
Transverse rms spot size (mm)	0.22	0.25
Bunch charge percentage (%)	0.004	0.002
Transverse coherence length (nm)	1.1	1.2
Rms bunch length (ps)	8.7	9.9

Electron beam qualities like energy spectra, divergence angle, and charge were determined prior to the filter stage. In this measurement, an IP wrapped in a 20-µm Al foil was placed opposite to the target [see Fig. 1b], providing spatially resolved detection of the electron beam. Typically in the conspicuous saturated ring

halo like the case shown in Figure 1b, an overall electron charge of around 30 pC was estimated to be confined or collimated within the saturated zone surround the wire target under our experimental parameters. It relays an electron beam with rms radius of 1.06 mm in the 3 mm-diameter entrance aperture. This is equivalent to a half-emitting divergence angle as small as 26 mrad that entered the filter stage. Approximately 36% electrons could enter this first entrance hole, namely about 10 pC ($\sim 6.3 \times 10^7$ electrons) could enter the filter stage under our experimental parameters.

We present the results for electron filter with the magnets set to 28 mT and a separation distance of 40 mm. The filter tube had 0.3 mm radius and a 135 mm-long drift length. Figure 4a displays a measured electron beam profile obtained in the absence of a sample. The spatial width of the electron beam could be well fitted by a Gaussian function with an FWHM of 0.27 mm. Owing to the weak laser intensity and the resultant small number of electrons in our experimental conditions, six shots were accumulated in the
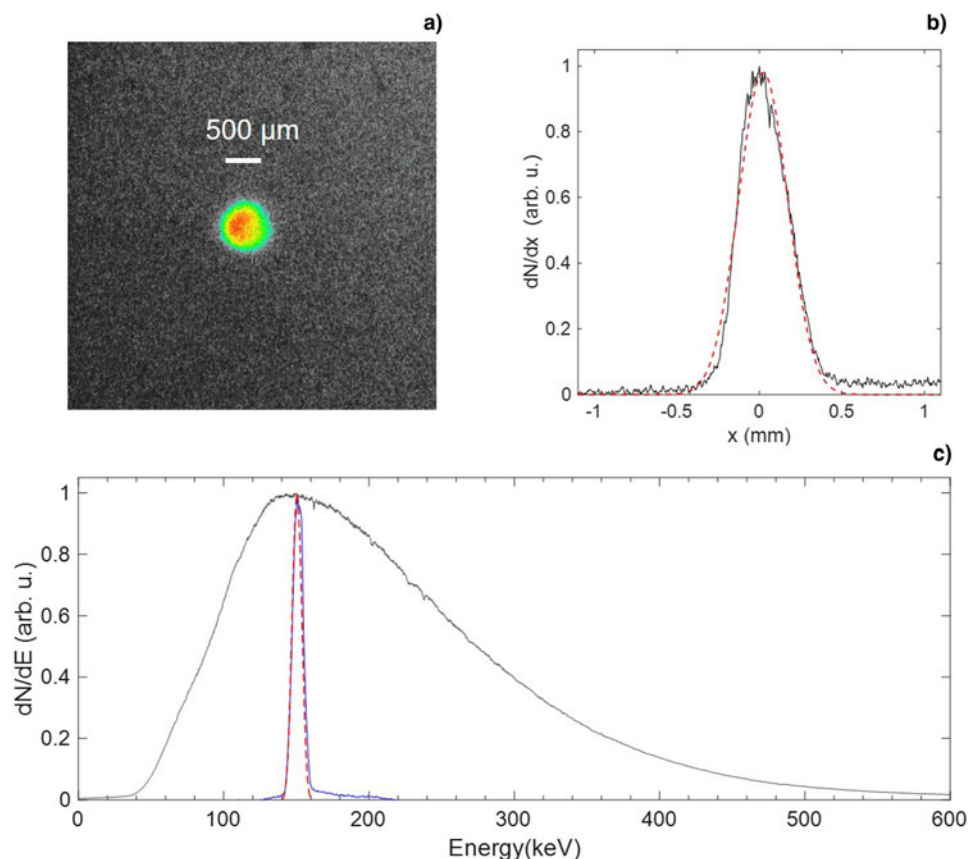
Fig. 4. (a) Obtained electron beam pattern at the exit of the filter tube without the sample present. (b) Horizontal beam profile from the measured pattern (black curve) and from ELEGANT simulations. (c) Normalized electron energy distribution before the filter stage (black curve) and that at the exit of the filter tube (blue curve). The dashed red line represents the calculated result.

total ∼6-fC electron charge estimated in this profile, indicating an average charge of ∼1 fC (∼6.3×10^3 electrons) in each electron pulse that arrived at the sample. In other words, approximately 0.01% portion of the relayed electrons were filtered by the filter tube for diffraction usage.

The energy distribution for electron beams either before or after the filter unit was measured with a magnetic spectrometer. The evident effect of energy narrowing could be seen in Figure 4c where the sharp blue curve represents the filtered electron spectrum in comparison to that before filtering (dark curve). The peak energy before or after the filter stage remained around 150 keV (or 419 keV/c in momentum). And the FWHM momentum spread related to these two places are 33 and 2.9%, respectively. The filtered energy changes with a different horizontal displacement of the filter tube to the wire axis. Hence, the broad initial energy spread provides an abundant source for electron diffraction in the 100–300 keV range. However, the energy distribution of the filtered electrons is not as desirably stable as for multishot experiments. Peak energy fluctuated up to ±30 keV from shot to shot. Possible reasons may arise from fluctuations in laser energy (∼2.5%) and alignment of the filter tube. Consequently, this scheme is considered to operate in a single-shot mode only provided that the stability problem had not been well-solved. Nevertheless, since an increase in laser intensity enhances collimated electrons in the central spot dramatically without a significant change in energy spread (Tokita *et al.*, 2011; Nakajima *et al.*, 2013), it suggests that increasing laser intensity could be one possible way to manifold the electron

charge that satisfies the requirement for single-shot in a few hundred keV range.

Note here expanded filter tube radius as well as shortened filter tube length were adopted in the experiment compared to the simulation parameters. The adjustment was a trade-off made between the transverse coherence and the low electron charge resultant from our modest laser intensity. Electron loss also took place in the alignment deviation of the wire with the tube axis as well as the inhomogeneity in electron distribution, magnetic field as compared to the uniform assumptions in the simulation. With experimental filter unit parameters, the simulation results predict electron beam profile in good agreement with the experimental one [Fig. 4b] with rms radius of $\sigma_x = 0.2$ mm. The produced transverse normalized emittance of the filtered electron beam is retrieved as $\varepsilon_{n,x} = 1.4 \times 10^{-1}$ mm mrad. The transverse coherence length L_c is then given by Eq. (1) with 0.57 nm, a value slightly bigger than the unit cell dimension of a single-crystal Au. However, a radical increase in L_c can be easily realized with adjustment in tube geometry and magnets with more initial electrons.

While the experiment shows a proof-of-principle demonstration employing a relatively low-energy laser system, there are still significant improvements that could be made toward single-shot electron diffraction, for example, (i) using a higher intensity laser pulse to create more collimated electrons; (ii) applying a more refined filter arrangement, such as a magnet combined with two apertures to simplify the whole setup to several centimeter scale (Tokita *et al.*, 2009); (iii) adopting more sensitive

detection devices such as an electron-multiplying charge-coupled camera or a scintillator plate to obtain a better resolved image; and (iv) combining the setup with laser-based electron pulse compression methods (Tokita *et al.*, 2010; van Oudheusden *et al.*, 2010) to further reduce the electron chirp. In addition, future studies in the geometric and plasma scale length parameters may also hint on methods that will improve electron qualities from the laser–plasma interaction.

Conclusion

In conclusion, we have demonstrated the optimization of the electron source from intense femtosecond laser interacting with a wire target. By manipulating the energy and spatial distributions of the electron pulse with two magnets served as the filter unit, we have demonstrated with numerical simulations the possibility of utilizing this approach for single-shot UED. A proof-of-principle experiment is conducted to provide an electron beam with 1 fC charge and transverse coherence length approaching 1 nm which indicates the scheme as a promising candidate for single-shot electron diffraction.

Furthermore, in comparison to the traditional dc-accelerated or laser-accelerated UED in the sub-MeV energy range, the extraordinary collimation ability of wire targets amounts to a novel, compact electron source that, unlike conventional sources, can deliver a vast number of electrons with extraordinary small divergence angle regardless of their energy. This wide energy spread from laser–solid interaction also enables the proposed scheme to work in an energy range of a few hundred keV range. Though stability, brightness, and transverse length of the filtered electron pulse still need to be increased to accommodate further applications. However, taking into consideration the modest low pulse energy used in our experiment, radical improvements could be expected through various approaches such as applying higher laser intensity to raise the collimated electron charge and using thinner filtering pinholes. Imaging can, meanwhile, be ameliorated using more effective filtering arrangements and detection devices. We, thus, believe that this development provides a competitive approach for observing irreversible ultrafast phenomena by UED in the near future.

References

Borland M (2000) *ELEGANT: A Flexible SDDS-Compliant Code for Accelerator Simulation. Advanced Photon Source LS-287*. IL, USA: Argonne National Lab.

Calendron A-L, Meier J, Hemmer M, Zapata LE, Reichert F, Cankaya H, Schimpf DN, Hua Y, Chang G, Kalaydzhyan A, Fallahi A, Matlis NH and Kaertner FX (2018) Laser system design for table-top X-ray light source. *High Power Laser Science and Engineering* 6, e12.

Couperus JP, Pausch R, Kohler A, Zarini O, Kramer JM, Garten M, Huebl A, Gebhardt R, Helbig U, Bock S, Zeil K, Debus A, Bussmann M, Schramm U and Irman A (2017) Demonstration of a beam loaded nanocoulomb-class laser wakefield accelerator. *Nature Communications* 8, 487.

Dann SJD, Baird CD, Bourgeois N, Chekhlov O, Eardley S, Gregory CD, Gruse JN, Hah J, Hazra D, Hawkes SJ, Hooker CJ, Krushelnick K,

Mangles SPD, Marshall VA, Murphy CD, Najmudin Z, Nees JA, Osterhoff J, Parry B, Pourmoussavi P, Rahul SV, Rajeev PP, Rozario S, Scott JDE, Smith RA, Springate E, Tang Y, Tata S, Thomas AGR, Thornton C, Symes DR and Streeter MJV (2019) Laser wakefield acceleration with active feedback at 5 Hz. *Physical Review Accelerators and Beams* 22, 041303.

Gibbon P (2004) *Short Pulse Laser Interactions with Matter*. Singapore: World Scientific Publishing Company, p. 153.

Gulde M, Schweda S, Storeck G, Maiti M, Yu HK, Wodtke AM, Schafer S and Ropers C (2014) Imaging techniques. Ultrafast low-energy electron diffraction in transmission resolves polymer/graphene superstructure dynamics. *Science* 345, 200–204.

Harb M, Ernstorfer R, Hebeisen CT, Sciaini G, Peng W, Dartigalongue T, Eriksson MA, Lagally MG, Kruglik SG and Miller RJ (2008) Electronically driven structure changes of Si captured by femtosecond electron diffraction. *Physical Review Letters* 100, 155504.

Leemans WP, Gonsalves AJ, Mao HS, Nakamura K, Benedetti C, Schroeder CB, Toth C, Daniels J, Mittelberger DE, Bulanov SS, Vay JL, Geddes CG and Esarey E (2014) Multi-GeV electron beams from capillary-discharge-guided subpetawatt laser pulses in the self-trapping regime. *Physical Review Letters* 113, 245002.

Malka V, Faure J, Glinec Y and Lifschitz AF (2006) Laser-plasma accelerator: status and perspectives. *Philosophical Transactions of the Royal Society A: Mathematical, Physical and Engineering Sciences* 364, 601–610.

Mordovanakis AG, Easter J, Naumova N, Popov K, Masson-Laborde PE, Hou B, Sokolov I, Mourou G, Glazyrin IV, Rozmus W, Bychenkov V, Nees J and Krushelnick K (2009) Quasimonoenergetic electron beams with relativistic energies and ultrashort duration from laser-solid interactions at 0.5 kHz. *Physical Review Letters* 03, 235001.

Musumeci P, Moody JT, Scoby CM, Gutierrez MS, Bender HA and Wilcox NS (2010) High quality single shot diffraction patterns using ultrashort megaelectron volt electron beams from a radio frequency photoinjector. *Review of Scientific Instruments* 81, 013306.

Nakajima H, Tokita S, Inoue S, Hashida M and Sakabe S (2013) Divergence-free transport of laser-produced fast electrons along a meter-long wire target. *Physical Review Letters* 110, 155001.

Otto MR, Rene de Cotret LP, Stern MJ and Siwick BJ (2017) Solving the jitter problem in microwave compressed ultrafast electron diffraction instruments: robust sub-50 fs cavity-laser phase stabilization. *Structural Dynamics* 4, 051101.

Schaeffer DB, Hofer LR, Knall EN, Heuer PV, Constantin CG and Niemann C (2018) A platform for high-repetition-rate laser experiments on the large plasma device. *High Power Laser Science and Engineering* 6, e17.

Sciaini G and Miller RJD (2011) Femtosecond electron diffraction: heralding the era of atomically resolved dynamics. *Reports on Progress in Physics* 74, 096101.

Srinivasan R, Lobastov VA, Ruan CY and Zewail AH (2003) Ultrafast Electron Diffraction (UED)—a new development for the 4D determination of transient molecular structures. *Helvetica Chimica Acta* 86, 1761–1799.

Tao Z, Zhang H, Duxbury PM, Berz M and Ruan C-Y (2012) Space charge effects in ultrafast electron diffraction and imaging. *Journal of Applied Physics* 111, 044316.

Thévenet M, Leblanc A, Kahaly S, Vincenti H, Vernier A, Quéré F and Faure J (2015) Vacuum laser acceleration of relativistic electrons using plasma mirror injectors. *Nature Physics* 12, 355–360.

Tian Y, Liu J, Wang W, Wang C, Deng A, Xia C, Li W, Cao L, Lu H, Zhang H, Xu Y, Leng Y, Li R and Xu Z (2012) Electron emission at locked phases from the laser-driven surface plasma wave. *Physical Review Letters* 109, 115002.

Tian Y, Liu J, Bai Y, Zhou S, Sun H, Liu W, Zhao J, Li R and Xu Z (2017) Femtosecond-laser-driven wire-guided helical undulator for intense terahertz radiation. *Nature Photonics* 11, 242–246.

Tokita S, Inoue S, Masuno S, Hashida M and Sakabe S (2009) Single-shot ultrafast electron diffraction with a laser-accelerated sub-MeV electron pulse. *Applied Physics Letters* 95, 111911.

Tokita S, Hashida M, Inoue S, Nishoji T, Otani K and Sakabe S (2010) Single-shot femtosecond electron diffraction with laser-accelerated

electrons: experimental demonstration of electron pulse compression. *Physical Review Letters* **105**, 215004.

Tokita S, Otani K, Nishoji T, Inoue S, Hashida M and Sakabe S (2011) Collimated fast electron emission from long wires irradiated by intense femtosecond laser pulses. *Physical Review Letters* **106**, 255001.

van Oudheusden T, de Jong EF, van der Geer SB, 't Root WPEMO, Luiten OJ and Siwick BJ (2007) Electron source concept for single-shot sub-100 fs electron diffraction in the 100 keV range. *Journal of Applied Physics* **102**, 093501.

van Oudheusden T, Pasmans PL, van der Geer SB, de Loos MJ, van der Wiel MJ and Luiten OJ (2010) Compression of subrelativistic space-charge-dominated electron bunches for single-shot femtosecond electron diffraction. *Physical Review Letters* **105**, 264801.

Wang X, Zgadzaj R, Fazel N, Li Z, Yi SA, Zhang X, Henderson W, Chang YY, Korzekwa R, Tsai HE, Pai CH, Quevedo H, Dyer G, Gaul E, Martinez M, Bernstein AC, Borger T, Spinks M, Donovan M, Khudik V, Shvets G, Ditmire T and Downer MC (2013) Quasi-monoenergetic laser-plasma acceleration of electrons to 2 GeV. *Nature Communications* **4**, 1988.